VIP Hydrated Proton

DOI: 10.1002/anie.200702201

Dynamics and Infrared Spectroscopy of the Protonated Water Dimer**

*Oriol Vendrell, Fabien Gatti, and Hans-Dieter Meyer**

Accurate infrared spectroscopy of protonated water clusters that are prepared in the gas phase has become possible in recent years,[1–6] thus opening the door to a deeper understanding of the properties of aqueous systems and the hydrated proton, which are of high interest in central areas of chemistry and biology. Several computational studies have appeared in parallel, providing a necessary theoretical basis for the assignment and understanding of the different spectral features.[6–10] It has been recently demonstrated that the $H_5O_2^+$ motif, also referred to as the Zundel cation, plays an important role in protonated water clusters of six or more water molecules and, together with the Eigen cation ($H_9O_4^+$), as a limiting structure of the hydrated proton in bulk water.[4,5,11] The importance of the hydrated proton and the amount of work devoted to the problem contrast with the fact that the smallest system in which a proton is shared between water molecules, $H_5O_2^+$, is not yet completely understood, and an explanation of the most important spectral signatures and the associated dynamics of the cluster is lacking.

Herein we report the simulation of the IR linear absorption spectrum of the $H_5O_2^+$ ion in the range 0–4000 cm^{-1} by state-of-the-art quantum-dynamical methods. We discuss the spectral signatures in terms of the underlying couplings and dynamics of the different degrees of freedom and compare our results to recent, accurate experiments on this system. For the first time the doublet signal at about 1000 cm^{-1} is fully reproduced, analyzed, and assigned. The doublet is found to arise from the coupling between the proton-transfer mode and low-frequency, large-amplitude displacements of both water molecules. Predictions are also made for the lowest-frequency part of the spectrum, which has not yet experimentally been accessed. Several important features of the system are analyzed for the first time, namely the degeneracy of some of the vibrational levels and the extreme anharmonicity of the wagging motions (pyramidalization) and relative internal rotation of the two water molecules. In doing so, we do not resort to any low-dimensional model of the system, but we treat it in its full dimensionality, that is, with $3N-6=15$ active internal coordinates (15D). The use of full dimensionality is found to be crucial in the reproduction of the complete absorption spectrum and dynamics. Our study provides a picture of the $H_5O^+_2$ system, and is extendable to larger aggregates, in which the clusters have to be viewed as highly anharmonic, flexible, coupled systems. From a methods perspective, we show that a full quantum-dynamical description of such a complex molecular system can still be achieved, providing explicative and predictive power and a very good agreement with available experimental data. In this respect, the reported simulations set a new state of the art in the *quantum-dynamical* description of an anharmonic, highly coupled molecular system of the size of the $H_5O_2^+$ ion. To account for the interatomic potential and the interaction with the radiation, we make use of the potential-energy surface (PES) and dipole-moment surfaces recently developed by Bowman and co-workers,[9] which constitute the most accurate ab initio surfaces available to date for this system.

The IR predissociation spectrum of the $H_5O_2^+$ ion has recently been measured in argon-solvate[3] and neon- and argon-solvate[6] conditions. It is expected that the photodissociation spectrum of the $H_5O_2^+{\cdot}Ne_1$ complex is close to the linear absorption spectrum of the bare cation.[6] This spectrum features a doublet structure in the region of 1000 cm^{-1} made of two well-defined absorptions at 928 and 1047 cm^{-1}. This doublet structure was not fully understood, although the highest-energy component was assigned to the asymmetric proton-stretch fundamental on the basis of the calculations by Bowman and co-workers.[6] Such an assignment was also proposed by Sauer and Dobler on the basis of classical-dynamics simulations.[10a] Low-frequency modes may also play an important role in combination with the proton-transfer fundamental. Such a possibility has already been suggested,[2,8,10] but just which modes would participate in such combinations, and how, is still a matter of discussion.

The Hamiltonian used in the simulation of $H_5O_2^+$ is expressed in a set of polyspherical coordinates based on the Jacobi vectors in Figure 1.[12] It was found that only after the introduction of such a curvilinear set of coordinates an adequate treatment of the anharmonic large-amplitude vibrations and torsions of the molecule becomes possible. The kinetic-energy operator is *exact* for $J=0$, and the derivation of its lengthy formula (674 terms) will be discussed in a forthcoming publication. The correctness of the operator implemented was checked by comparison with data generated by the TNUM program.[13] The internal coordinates used are:

[*] Dr. O. Vendrell, Prof. Dr. H.-D. Meyer
Theoretische Chemie
Physikalisch-Chemisches Institut
Universität Heidelberg
Im Neuenheimer Feld 229, 69120 Heidelberg (Germany)
Fax: (+49) 6221-54-5221
E-mail: hans-dieter.meyer@pci.uni-heidelberg.de
Homepage: http://www.pci.uni-heidelberg.de/tc/usr/dieter
Dr. F. Gatti
CTMM, Institut Charles Gerhardt, UMR 5253
CC 014, Université Montpellier II
34095 Montpellier, Cedex 05 (France)

[**] We thank Prof. J. Bowman for providing the potential-energy routine, D. Lauvergnat for performing the TNUM calculations, and the Scientific Supercomputing Center Karlsruhe for generously providing computer time. O.V. is grateful to the Alexander von Humboldt Foundation for financial support.

Supporting information for this article is available on the WWW under http://www.angewandte.org or from the author.

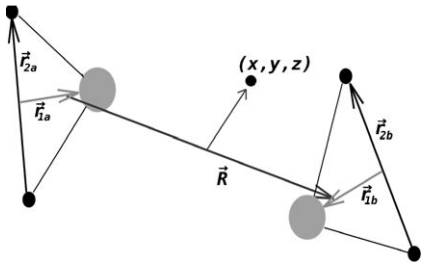

Figure 1. The geometry of $H_5O_2^+$ as described by six Jacobi vectors. The set of internal coordinates corresponds to the length of these vectors and relative angles. The *z* direction of the central proton is parallel to $\vec{R}$.

the distance between the centers of mass of both water molecules (R), the position of the central proton with respect to the center of mass of the water dimer (x,y,z), the Euler angles defining the relative orientation between the two water molecules (wagging or pyramidalization: γ_a,γ_b; rocking: β_a,β_b; internal relative rotation: α), and the Jacobi coordinates, which account for the particular configuration of each water molecule ($r_{1(a,b)},r_{2(a,b)},\theta_{(a,b)}$), where r_{1x} is the distance between the oxygen atom and the center of mass of the corresponding H_2 fragment, r_{2x} is the H–H distance, and θ_x is the angle between these two vectors. These internal coordinates are body-fixed (BF), such that the water–water distance vector $\vec{R}$ points along the BF *z* axis. These coordinates have the great advantage of leading to a much more decoupled representation of the PES than a normal-mode-based Hamiltonian. The quantum-dynamical problem is solved in the time-dependent picture by using the multiconfiguration time-dependent Hartree method (MCTDH).[14,15] The potential-energy surface has been represented by a cut high-dimensional model representation (cut-HDMR).[16,17]

In Figure 2 probability-density projections on the wagging coordinates are shown for the ground vibrational state (g_0), as well as for one of the two fundamental states (w_{1a},w_{1b}) of the wagging modes, which are degenerate vibrational states with an energy of 106 cm^{-1}. The w_3 state (see below for definition) is shown in Figure 2c, and it plays a major role owing to its coupling to the proton-transfer mode, as will be discussed later.

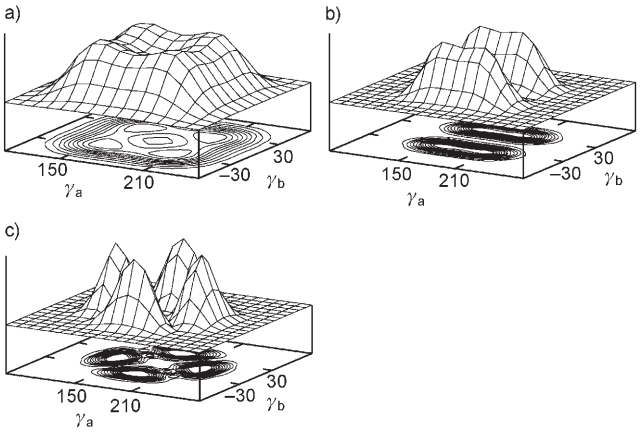

Figure 2. a) Probability density of a) the ground vibrational state, b) the first, and c) the third wagging-mode states projected onto the wagging coordinates γ_a and γ_b.

The probability density of the wagging coordinates in g_0 (Figure 2a) presents four maxima in which the wagging angle is about 30° with respect to the planar conformation for each water molecule. The probability for one or both water molecules of being found in a planar conformation is almost as high as the probability of being found in a pyramidal conformation. This result means that $H_5O_2^+$ interconverts already at $T=0$ K, owing to the zero-point energy, between equivalent absolute-minimum-energy structures in which both water molecules are found in a pyramidal conformation. Four equivalent minimum-energy structures are accessible through wagging motions. The number of accessible equivalent minima at $T=0$ doubles to eight since the relative rotation of both water molecules (α coordinate) has also been found to be allowed through a low-energy barrier.

The energies of the next three wagging-mode states (w_2,w_3,w_4) are 232, 374, and 422 cm^{-1}, respectively. In a harmonic limit these states can be represented by the kets $|11\rangle$, $(|20\rangle-|02\rangle)/\sqrt{2}$, and $(|20\rangle+|02\rangle)/\sqrt{2}$, respectively, where the $|ab\rangle$ notation signifies the quanta of excitation in the wagging motions of water molecules *a* and *b*. The degeneracy between w_2, w_3, and w_4 is broken owing to anharmonicity. In a harmonic approximation the energies of the two lowest wagging fundamentals w_{1a} and w_{1b} are about 300 cm^{-1} larger than our result and do not account for their degeneracy, as harmonic modes are constructed by taking as a reference only one of the equivalent absolute minima. The system, however, interconverts between eight equivalent C_2 structures and other stationary points through low-energy barriers (wagging motions and internal rotation), which leads to a highly symmetric ground-state wavefunction. Other vibrational states have been computed which are related to the internal rotation, rockings, and water–water stretching modes. They will be reported and discussed in a forthcoming publication.

Figure 3 presents the IR predissociation spectrum of the $H_5O_2^+$·Ne complex[6] and the simulated spectrum of $H_5O_2^+$ in the range 700–1900 cm^{-1}. The simulated spectrum is obtained in the time-dependent picture by Fourier transformation of the autocorrelation of a dipole-operated intial state

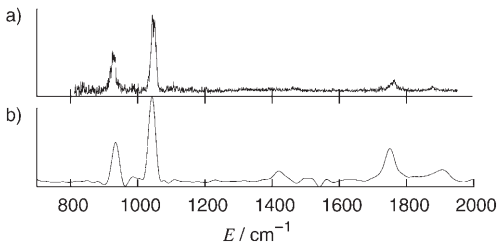

Figure 3. a) Predissociation spectrum of the $H_5O_2^+$·Ne complex;[6] b) quantum-dynamical simulation. The spectral resolution is given by the Fourier transform. Owing to the finite propagation time, a finite resolution of about 30 cm^{-1} is obtained.

[Eq. (1)],[18] where E_0 is the ground-state energy and $|\Psi_{\mu,0}\equiv\hat{\mu}\,|\Psi_0\rangle$. The simulated spectrum shows a good agreement with the experimental spectrum. The agreement on the doublet structure around 1000 cm^{-1} is very good, and the position of the doublet at 1700–1800 cm^{-1} is also in good agreement, despite the relative intensities being larger in the simulation.

$$I(E)=\frac{E}{3\epsilon\varepsilon\hbar^2}\int_0^\infty \exp(i(E+E_0)t/\hbar)\langle\Psi_{\mu,0}|\exp(-i\hat{H}t/\hbar)|\Psi_{\mu,0}\rangle dt \qquad (1)$$

The simulated spectrum in the range between 0 and 4000 cm^{-1} is depicted in Figure 4. The region below 700 cm^{-1} has not yet been accessed experimentally. Direct absorption of the wagging motions, excited by the perpendicular components of the field, appears in the range 100–200 cm^{-1}. The doublet starting at 1700 cm^{-1} is clearly related to bending motions of the water molecules, but its exact nature is still to be addressed. The simulated spectrum also shows the absorptions of the OH stretchings starting at 3600 cm^{-1}.

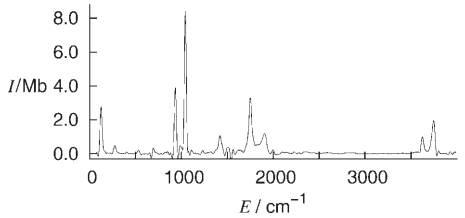

Figure 4. Quantum-dynamical simulated spectrum in the range 0–4000 cm^{-1}. Absorption is given in megabarns (Mb).

The doublet absorption at about 1000 cm^{-1} and the related underlying dynamics deserve a deeper analysis. Owing to the high density of the states, it was not possible to obtain the fully converged states, but reasonably good approximations to the wavefunctions of the low-energy ($|\Psi_l^d\rangle$, 930 cm^{-1}) and high-energy ($|\Psi_h^d\rangle$, 1021 cm^{-1}) eigenstates of the doublet were computed. Even though these wavefunctions contain all the possible information on the two states, their direct analysis becomes complex owing to the high dimensionality of such objects. To obtain a fundamental understanding of the observed bands, zeroth-order states $|\Phi_z\rangle$ and $|\Phi_{R,w_3}\rangle$ were constructed, where $|\Phi_z\rangle$ is characterized by one quantum of excitation in the proton-transfer coordinate, whereas $|\Phi_{R,w_3}\rangle$ is characterized by one quantum in the water–water stretch and two quanta in the wagging motion. These states were constructed by using the $\hat{z}$ operator on the ground state: $|\Phi_z\rangle=\hat{z}\,|\Psi_0\rangle N$, where N is a normalization constant, and by using the $(\hat{R}-R_0)$ operator on the third excited wagging state w_3: $|\Phi_{R,w_3}\rangle=(\hat{R}-R_0)\,|\Psi_{w_3}\rangle N$. The two eigenstates of the doublet were then projected onto these zeroth-order states. The corresponding overlaps read: $|\langle\Phi_z\,|\,\Psi_l^d\rangle|^2=0.20$, $|\langle\Phi_{R,w_3}|\,\Psi_l^d\rangle|^2=0.53$ and $|\langle\Phi_z\,|\,\Psi_h^d\rangle|^2=0.48$, $|\langle\Phi_{R,w_3}|\,\Psi_h^d\rangle|^2=0.12$.

One should take into account that these numbers depend on the exact definition of the zeroth-order states, which is not unique. However, they provide a clear picture of the nature of the doublet: The low-energy band has the largest contribution from the combination of the water–water stretch and the third wagging excitation (see Figure 2c), whereas the second-largest contribution is the proton-transfer motion. For the high-energy band the importance of these two contributions is reversed. Thus, the doublet may be regarded as a Fermi resonance between two zeroth-order states which are characterized by (R,w_3) and (z) excitations, respectively. The reason why the third wagging excitation plays an important role in the proton-transfer doublet is understood by inspecting Figure 2c and Figure 5. The probability density of the w_3 state has four maxima, each of which corresponds to a planar conformation of H_2O–H^+ (H_3O^+ character) for one of the water molecules, and a bent conformation (H_2O character) in which a lone-pair H_2O orbital forms a hydrogen bond with the central proton. When the proton oscillates between the two water molecules, the two conformations exchange their characters accordingly. Thus, the asymmetric wagging mode (w_3, 374 cm^{-1}) combines with the water–water stretching motion (R, 550 cm^{-1}) to reach an energy close to the natural absorption frequency of the proton transfer. As a consequence, the low-frequency wagging (or pyramidalization) motion of the water molecules becomes strongly coupled to the higher-frequency, spectroscopically active proton-transfer motion, and this coupling leads to the characteristic doublet feature of the IR spectrum.

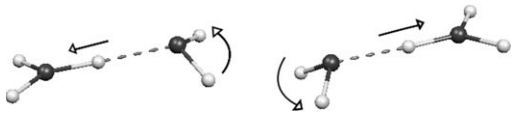

Figure 5. Two most important coupled motions (wagging and proton transfer) responsible for the doublet at 1000 cm^{-1}.

In conclusion, we report a simulation of the dynamics and IR absorption spectrum of the $H_5O_2^+$ cation by quantum-dynamical methods in the full spectral range 0–4000 cm^{-1}. The spectrum is directly comparable to available and future experiments on this system. We discuss some important features of the protonated water dimer which have remained until now elusive. The flexible, anharmonic nature of the cluster is presented and analyzed, and the doublet-band absorption around 1000 cm^{-1} is fully reproduced and explained in terms of coupling of the proton-transfer motion to wagging (w_3) and water–water stretching (R). These calculations constitute an avenue for a detailed quantum-dynamical description of larger clusters and provide important fundamental information on the spectroscopy and dynamics of protonated aqueous systems and the hydrated proton.

Received: May 18, 2007
Published online: August 3, 2007

Keywords: IR spectroscopy · molecular dynamics · proton transport · quantum dynamics · water clusters

[1] K. R. Asmis, N. L. Pivonka, G. Santambrogio, M. Brummer, C. Kaposta, D. M. Neumark, L. Woste, *Science* **2003**, *299*, 1375 – 1377.
[2] T. D. Fridgen, T. B. McMahon, L. MacAleese, J. Lemaire, P. Maitre, *J. Phys. Chem. A* **2004**, *108*, 9008 – 9010.
[3] J. M. Headrick, J. C. Bopp, M. A. Johnson, *J. Chem. Phys.* **2004**, *121*, 11523 – 11526.
[4] J.-C. Jiang, Y.-S. Wang, H.-C. Chang, S. H. Lin, Y. T. Lee, G. Niedner-Schatteburg, H.-C. Chang, *J. Am. Chem. Soc.* **2000**, *122*, 1398 – 1410.
[5] J. M. Headrick, E. G. Diken, R. S. Walters, N. I. Hammer, R. A. Christie, J. Cui, E. M. Myshakin, M. A. Duncan, M. A. Johnson, K. D. Jordan, *Science* **2005**, *308*, 1765 – 1769.
[6] N. I. Hammer, E. G. Diken, J. R. Roscioli, M. A. Johnson, E. M. Myshakin, K. D. Jordan, A. B. McCoy, J. M. Bowman, S. Carter, *J. Chem. Phys.* **2005**, *122*, 244301.
[7] M. V. Vener, O. Kühn, J. Sauer, *J. Chem. Phys.* **2001**, *114*, 240 – 249.
[8] J. Dai, Z. Bacic, X. C. Huang, S. Carter, J. M. Bowman, *J. Chem. Phys.* **2003**, *119*, 6571 – 6580.
[9] X. Huang, B. J. Braams, J. M Bowman, *J. Chem. Phys.* **2005**, *122*, 044308.
[10] a) J. Sauer, J. Dobler, *ChemPhysChem* **2005**, *6*, 1706 – 1710; b) M. Kaledin, A. L. Kaledin, J. M. Bowman, *J. Phys. Chem. A* **2006**, *110*, 2933 – 2939.
[11] a) D. Marx, M. Tuckerman, J. Hutter, M. Parrinello, *Nature* **1999**, *397*, 601 – 604; b) N. Agmon, *Isr. J. Chem.* **1999**, *39*, 493 – 502.
[12] F. Gatti, *J. Chem. Phys.* **1999**, *111*, 7225.
[13] D. Lauvergnat, A. Nauts, *J. Chem. Phys.* **2002**, *116*, 8560.
[14] a) U. Manthe, H.-D. Meyer, L. S. Cederbaum, *J. Chem. Phys.* **1992**, *97*, 3199 – 3213; b) M. H. Beck, A. Jäckle, G. A. Worth, H.-D. Meyer, *Phys. Rep.* **2000**, *324*, 1 – 105.
[15] A brief description of the MCTDH method is given in the Supporting Information.
[16] a) J. M. Bowman, S. Carter, X. Huang, *Int. Rev. Phys. Chem.* **2003**, *22*, 533 – 549; b) G. Y. Li, C. Rosenthal, H. Rabitz, *J. Phys. Chem. A* **2001**, *105*, 7765 – 7777.
[17] A brief discussion on the construction of the potential-energy representation for the quantum-dynamical simulations is provided in the Supporting Information. A more detailed discussion on the construction and accuracy of the potential-energy representation will be given in a forthcoming publication.
[18] G. G. Balint-Kurti, R. N. Dixon, C. C. Marston, *J. Chem. Soc. Faraday Trans.* **1990**, 1741.

